

# Quantum phase transitions in attractive extended Bose-Hubbard Model with three-body constraint

Yung-Chung Chen, Kwai-Kong Ng, and Min-Fong Yang  
*Department of Physics, Tunghai University, Taichung 40704, Taiwan*  
 (Dated: July 27, 2018)

The effect of nearest-neighbor repulsion on the ground-state phase diagrams of three-body constrained attractive Bose lattice gases is explored numerically. When the repulsion is turned on, in addition to the uniform Mott insulating state and two superfluid phases (the atomic and the dimer superfluids), a dimer checkerboard solid state appears at unit filling, where *boson pairs* form a solid with checkerboard structure. We find also that the first-order transitions between the uniform Mott insulating state and the atomic superfluid state can be turned into the continuous ones as the repulsion is increased. Moreover, the stability regions of the dimer superfluid phase can be extended to modest values of the hopping parameter by tuning the strength of the repulsion. Our conclusions hence shed light on the search of the dimer superfluid phase in real ultracold Bose gases in optical lattices.

Spectacular progress both in theories and experiments has recently been made on ultracold atomic and molecular gases in optical lattices. Owing to the remarkable control over physical parameters, ultracold gases offer opportunities to simulate the physics of strongly correlated systems in regimes which are not easily accessible to solid-state materials. As a result, they provide very clean and tunable systems in the search for exotic quantum phases and in probing quantum critical behaviors around these phases.<sup>1</sup> For instance, successful experimental realization of the superfluid-Mott transition for ultracold bosons in an optical lattice<sup>2</sup> has paved the way for studying other strongly correlated phases in various lattice models.

Very recently, it was suggested that intriguing quantum critical behaviors could occur in attractive bosonic lattice gases with three-body on-site constraint.<sup>3,4</sup> The on-site constraint can arise naturally due to large three-body loss processes,<sup>5,6</sup> and it stabilizes the attractive bosonic systems against collapse. Such three-body constrained systems can be realized also in Mott insulating states of ultracold spin-one atoms at unit filling.<sup>7</sup> As found by the authors in Ref. 3, a dimer superfluid (DSF) phase consisting of the condensation of boson pairs can be realized under sufficiently strong attraction. According to their analysis, the transitions between the DSF phase and the conventional atomic superfluid (ASF) state are proposed to be of Ising-like at unit filling and driven first-order by fluctuations via the Coleman-Weinberg mechanism<sup>8</sup> at other fractional fillings. Later investigation focuses on the nature of the superfluid-insulator transitions.<sup>4</sup> It is shown that, while the Mott-insulator (MI) to DSF transitions are always of second order, the continuous MI-ASF transitions can be preempted by first-order ones and interesting tricritical points can thus appear on the MI-ASF phase boundaries. The conclusions obtained in Refs. 3 and 4 are partly supported by a recent numerical study employing stochastic series expansion (SSE) quantum Monte Carlo (QMC) method implemented with a generalized directed loop algorithm.<sup>9</sup> In particular, the existence of a tricritical point along the saturation transition line is verified. However, the nature of MI-DSF

transitions is not examined in their QMC work.

In the present work, the effect of the nearest-neighbor mutual repulsion on the ground-state phase diagrams of three-body constrained attractive lattice bosons is investigated by means of exact diagonalizations (ED). The systems under consideration are described by the extended Bose-Hubbard model with a three-body constraint  $a_i^{\dagger 3} \equiv 0$  on square lattices,

$$H = H_{\text{EBH}} - \mu \sum_i n_i, \quad (1)$$

$$H_{\text{EBH}} = -t \sum_{\langle i,j \rangle} a_i^{\dagger} a_j + \frac{U}{2} \sum_i n_i (n_i - 1) + V \sum_{\langle i,j \rangle} n_i n_j.$$

Here,  $a_i$  ( $a_i^{\dagger}$ ) is the bosonic annihilation (creation) operator at site  $i$ ,  $t$  is the nearest-neighbor hopping integral,  $U < 0$  is the on-site two-body attraction ( $|U| \equiv 1$  as the energy unit), and  $\mu$  is the chemical potential.  $V > 0$  denotes the nearest-neighbor repulsion, which can come from the dipole-dipole interactions of the dipolar bosons polarized perpendicularly to the lattice plane by truncating it at the nearest-neighbor distance. For the discussions of possible experimental realizations on the present model, we refer to Ref. 10 and references therein. The averaged particle density is denoted by  $n$  and periodic boundary conditions are assumed. Our main results are summarized in Fig. 1. When  $V \neq 0$ , in addition to the MI and two superfluid phases mentioned above, a dimer checkerboard solid (DCS) state consisting of the checkerboard arrangement of *boson pairs* emerges and occupies the middle part of the phase diagram in the small- $t$  limit. The DSF states now appear only in between the uniform MI and the DCS states. Moreover, finite repulsion has interesting effects on the MI-superfluid transitions also. Because a modest nearest-neighbor repulsion can avoid cluster formation and then will suppress phase separation, we observe that the segments of the first-order MI-ASF transitions on phase boundaries of either the  $n = 0$  or the  $n = 2$  MI states (denoted by thick blue dashed lines in Fig. 1) can shrink to zero as  $V$  is increased. Same conclusion has been reached in other context.<sup>11</sup> Besides,

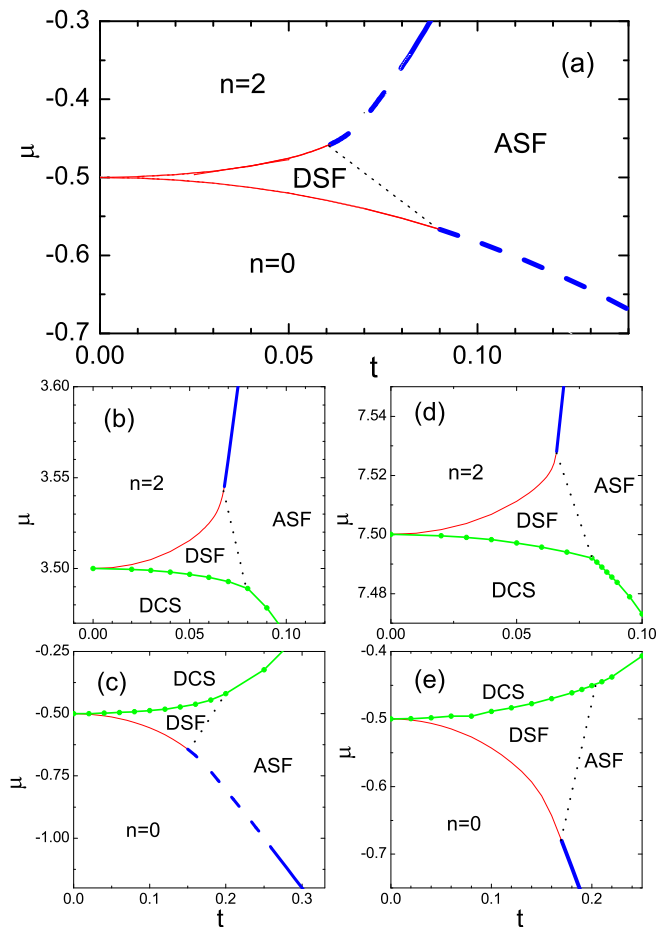


FIG. 1: (Color online) Ground-state phase diagram obtained by ED with (a)  $V = 0$ , (b)(c)  $V = 1/2$ , and (d)(e)  $V = 1$ . The thin red solid lines indicate the continuous MI-DSF transitions, and the thick blue solid (dashed) lines show the continuous (first-order) MI-ASF transitions. The phase boundaries of the DCS state are denoted by the green solid circles (lines are guides to the eye). The error bar of the determined phase boundaries is smaller than the width of the lines or the size of the symbols. The schematic phase boundaries between the ASF and the DSF phases are added as the thin dotted lines for clarity.

our findings show that the phase boundaries of the MI-DSF transitions (denoted by thin red solid lines in Fig. 1) and therefore the stability region of the DSF phase in the low-density limit can be extended to modest hopping parameters  $t$  upon tuning  $V$ , such that experimental exploration of this interesting state becomes more feasible. Our work hence provides a useful guide to the experimental search of the DSF phase and the associated quantum phase transitions in ultracold Bose gases in optical lattices.

The details of our analysis are explained below. According to the discussions in Ref. 11, one can determine the phase boundaries of either the  $n = 0$  MI state (i.e., the empty state) or the  $n = 2$  MI state (i.e., the completely filled state) for a given  $t$  as follows. For the tran-

sitions out of the  $n = 0$  MI state, we calculate the excitation energies (relative to the  $n = 0$  state)  $E(1) - \mu$ ,  $E(2) - 2\mu$ , and  $E(4) - 4\mu$  of the lowest states within the subspaces of fixed total particle numbers  $N_p = 1, 2$ , and 4, respectively. Here  $E(N_p)$  denotes the lowest excitation energy of  $H_{\text{EBH}}$  within the fixed  $N_p$  subspace. From these quantities, the two- and the four-particle binding energies,  $\Delta_{2p} = E(2) - 2E(1)$  and  $\Delta_{4p} = E(4) - 2E(2)$ , can be obtained. For a given value of the hopping parameter  $t$ , if both  $\Delta_{2p}$  and  $\Delta_{4p}$  are positive, there exists no bound states and the energy gap of the single-particle state closes first upon increasing the chemical potential  $\mu$ . This leads to a continuous MI-ASF transition at  $\mu_{c,0\text{MI-ASF}} = E(1)$ .<sup>12</sup> When  $\Delta_{2p} < 0$  but  $\Delta_{4p} > 0$ , instead, a bound state of two particles appears and its gap closes first. Thus a continuous MI-DSF transition will occur at  $\mu_{c,0\text{MI-DSF}} = E(2)/2$ . Aside from these two possibilities, the condition of  $\Delta_{4p} < 0$  gives a precursor of instability of boson pairs towards cluster formation. That is, phase separation emerges and a first-order transition will be observed in varying  $\mu$ . In the present ED analysis, we estimate the first-order transition point by  $E(4)/4$ , which provides an upper bound of the exact value. Similar discussions apply to the transitions out of the  $n = 2$  MI state, where the holes created from the  $n = 2$  state take the role played by the particles discussed previously. We remind that the first-order transition points estimated by the four-hole excitation energies will be instead lower bounds of the exact values along the saturation transition line.

Here distinct MI-superfluid transitions are determined by the above method for systems of  $N_s = 10 \times 10$  sites. The analysis for the  $V = 1/2$  case is described below for illustration. The results of various binding energies as functions of hopping parameter  $t$  for this  $V$  are presented in Fig. 2. As seen from Fig. 2(b), there is a finite region of  $t$  within which  $\Delta_{4p} < 0$ . It implies that, on the phase boundary of the  $n = 0$  state, the continuous MI-DSF (for  $\Delta_{2p} < 0$  but  $\Delta_{4p} > 0$ ) and continuous MI-ASF (for both  $\Delta_{2p}, \Delta_{4p} > 0$ ) transitions are separated by first-order MI-ASF transitions for  $0.15 \lesssim t \lesssim 0.26$ . On the contrary, the two continuous MI-superfluid transitions on the phase boundary of the  $n = 2$  state should meet directly at  $t \approx 0.068$ . The transition points  $\mu_c$  for a given  $t$  can be determined by using the excitation energies  $E(N_p)$  as explained above.<sup>13</sup> According to our ED calculations, for  $V = 1/2$ , the continuous  $n = 2$  MI-DSF transitions end at  $(t_E, \mu_E) \simeq (0.068, 3.55)$ , while  $(t_E, \mu_E) \simeq (0.15, -0.64)$  for that of the continuous  $n = 0$  MI-DSF transition line. There exists also a tricritical point  $(t_T, \mu_T) \simeq (0.26, -1.04)$  on the  $n = 0$  MI-ASF transition line separating the continuous from the first-order ones.

We now turn to the discussions on the phase boundaries of the DCS state. Due to the effect of the nearest-neighbor repulsion  $V$ , *boson pairs* can form a solid with checkerboard structure at unit filling  $n = N_p/N_s = 1$  and lead to the DCS state. In the zero-hopping limit,

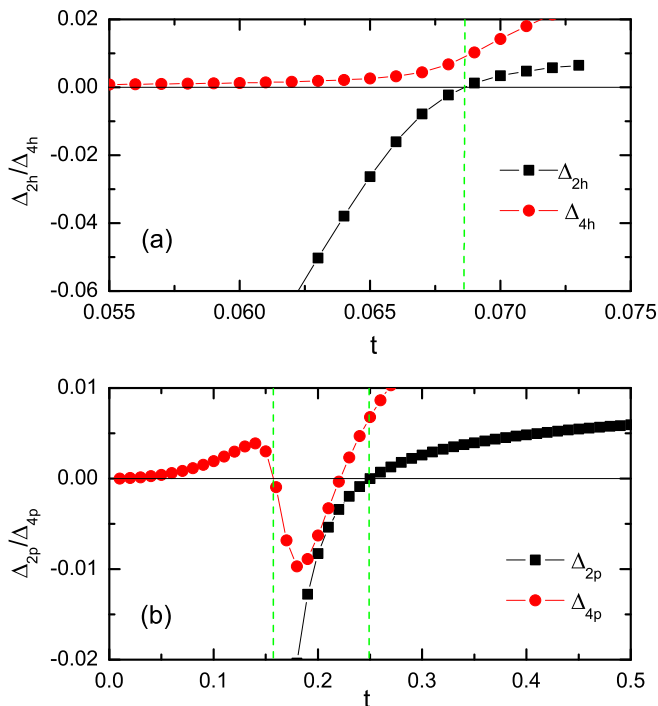


FIG. 2: (Color online) (a) Two- and four-hole binding energies,  $\Delta_{2h}$  and  $\Delta_{4h}$ , around the  $n = 2$  state and (b) two- and four-particle binding energies,  $\Delta_{2p}$  and  $\Delta_{4p}$ , around the  $n = 0$  state as functions of  $t$  for  $V = 1/2$  and  $N_s = 10 \times 10$ . The dashed lines separate the transitions of different characters.

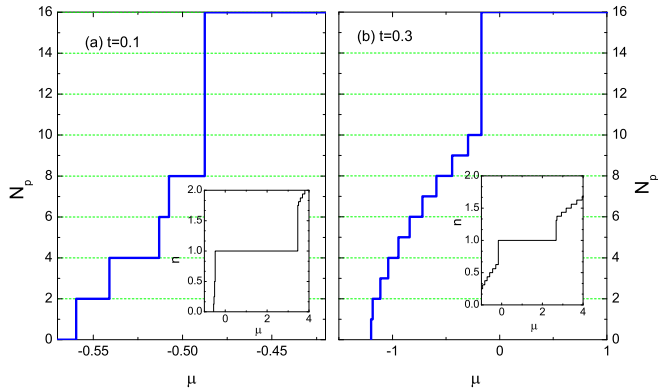


FIG. 3: (Color online) Total particle numbers  $N_p$  as functions of chemical potential  $\mu$  for (a)  $t = 0.1$  and (b)  $t = 0.3$  with  $V = 1/2$  and system sizes  $N_s = 4 \times 4$ . The insets illustrate the complete changes in particle density  $n$  from the  $n = 0$  to the  $n = 2$  states as  $\mu$  increases.

this DCS state can be stabilized when  $-1/2 < \mu < -1/2 + 2zV$  with the coordination number  $z = 4$  for square lattices. The DCS state can melt into the DSF or the ASF states under increasing hopping, and its stability region in  $\mu$  is expected to reduce to zero as  $t$  increases. This picture is supported by our numerical calculations as seen in Fig. 1. Due to the limitation in numerics, the phase boundaries of the DCS state are estimated from

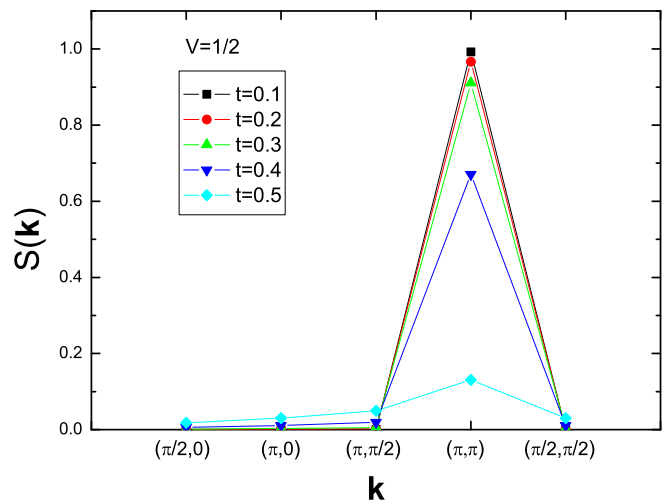


FIG. 4: (Color online) Static structure factor  $S(\mathbf{k})$  of the  $n = 1$  states for various  $t$ 's with  $V = 1/2$  and  $N_s = 4 \times 4$ .

the  $n = 1$  plateaus in the  $\mu$ - $n$  plots for different  $t$ 's with system sizes of  $N_s = 4 \times 4$ . For illustration, total particle numbers  $N_p$  and the particle density  $n$  as functions of chemical potential  $\mu$  for two different values of  $t$ 's with  $V = 1/2$  are presented in Fig. 3. The large plateaus at  $n = 1$  in the  $\mu$ - $n$  plots clearly indicate the presence of the DCS state. Two ends of the plateau give the melting transition points in  $\mu$  for a given  $t$ , as depicted in Fig. 1. Moreover, distinct characters in various transitions can be revealed by the way in which the total particle number  $N_p$  changes upon varying the chemical potential  $\mu$ .<sup>11</sup> In the conventional ASF phase, the number of particles will increase by 1 when the chemical potential is increased. However, in the DSF phase, only pairs of bosons appear in the system due to the presence of a pairing gap. Thus adding a single boson is forbidden and the jumps in the particle number by 2 will be observed as  $\mu$  is varied. Besides forming pairs, bosons can become unstable towards cluster formation such that the particle number jumps by a finite amount in the course of tuning  $\mu$ . This corresponds to a first-order transition under the change in the chemical potential. As shown in Fig. 3, for  $t = 0.1$ , the system evolves across a continuous MI-DSF transition from the  $n = 0$  state to the DSF state, and then follows a first-order transition to the DCS state. For larger  $t$  (say,  $t = 0.3$ ), the state after the continuous transition from the  $n = 0$  MI state becomes the ASF one instead. Adding more bosons by further increasing  $\mu$ , the system can again follow a first-order transition to the DCS state.

To provide support on the nature of the DCS states within the  $n = 1$  plateaus in the  $\mu$ - $n$  curves, the static structure factors  $S(\mathbf{k}) = (1/N_s^2) \langle |\sum_j n_j e^{i\mathbf{k}\cdot\mathbf{r}_j}|^2 \rangle$  of the  $n = 1$  states for several hopping parameters  $t$ 's with  $V = 1/2$  and system size  $N_s = 4 \times 4$  are shown in Fig. 4. It is found that the static structure factors do have peaks at the wave vector  $\mathbf{k} = (\pi, \pi)$  and thus signal the checkerboard pattern of the boson pairs. As observed

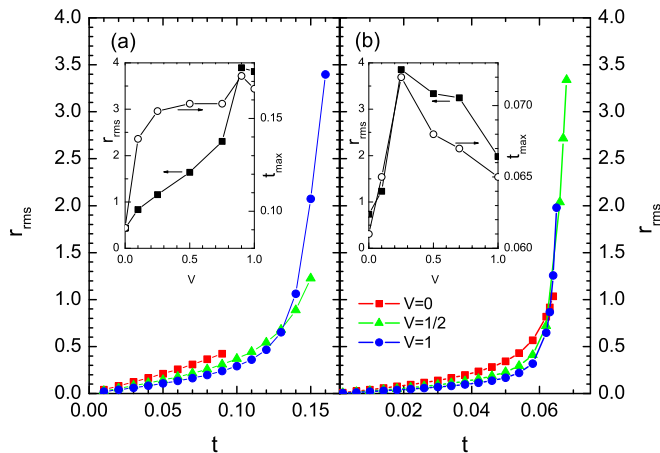


FIG. 5: (Color online) Root-mean-square separation  $r_{\text{rms}}$  of the (a) particle (b) hole pairs on  $N_s = 10 \times 10$  square lattices as functions of  $t$  for various repulsions  $V$ . Insets:  $r_{\text{rms}}$  and maximal extent  $t_{\text{max}}$  in hopping integral for the MI-DSF transitions as functions of  $V$ .

from Fig. 4, when  $t$  is increased, the peak value  $S(\pi, \pi)$  of the structure factor will decrease from its classical value  $S(\pi, \pi) = 1$  at  $t = 0$ . This indicates the quantum melting of the DCS state into the DSF or the ASF states under increasing hopping.

Some further microscopic details can be uncovered by the ED calculations. Similar to the counterpart of fermion pairing, a smooth crossover from the on-site pairs to the loosely bound pairs may occur also in the present attractive boson systems as the hopping parameter  $t$  increases. In Fig. 5, evidences supporting this expectation are presented. Here the coherence length of the boson pairs is estimated by the root-mean-square sep-

aration  $r_{\text{rms}} \equiv \sqrt{\langle r^2 \rangle}$ ,<sup>15,16</sup> which is evaluated under the ground state of a single pair within the two-particle or the two-hole subspaces. Our results show rapid but smooth crossovers from the tightly bound molecules to the loosely bound pairs, as long as the DSF phase can be stabilized up to modest values of  $t$  (say, the  $V = 1$  case for the particle pairs and the  $V = 1/2$  case for the hole pairs). The general dependence on the repulsion  $V$  of the maximal extent  $t_{\text{max}}$  in hopping integral for the stable DSF state in the low-density limit and the corresponding  $r_{\text{rms}}$  is shown in the insets of Fig. 5. We find that larger  $t_{\text{max}}$ 's in general lead to longer  $r_{\text{rms}}$ 's. The dependence of  $t_{\text{max}}$  and  $r_{\text{rms}}$  on  $V$  is found to be nonmonotonic, and their functional forms shows asymmetry between the cases of the particle and the hole pairs. Our conclusions presented in Figs. 1 and 5 should be of help in determining optimal experimental settings in the search of the DSF phase in ultracold Bose gases in optical lattices.

In summary, the ground-state phase diagrams of the three-body constrained extended Bose-Hubbard model for various repulsions are investigated. Large plateaus at  $n = 1$  in the  $\mu$ - $n$  curves which show the DCS states are observed. Finite repulsions modify the MI-superfluid transitions also. We find that the repulsion  $V$  can change the first-order MI-ASF transitions into the continuous ones and the stability regions of the DSF phase can be tuned by  $V$ . Therefore, carefully adjusting system parameters into the suggested parameter regime are necessary to find experimentally the interesting DSF phase in real ultracold Bose gas in optical lattices.

Y.-C.C., K.-K.N., and M.-F.Y. thank the National Science Council of Taiwan for support under Grant No. NSC 99-2112-M-029-002-MY3, NSC 97-2112-M-029-003-MY3, and NSC 99-2112-M-029-003-MY3, respectively.

<sup>1</sup> M. Lewenstein, A. Sanpera, V. Ahufinger, B. Damski, A. Sen, and U. Sen, *Adv. Phys.* **56**, 243 (2007); I. Bloch, J. Dalibard, and W. Zwerger, *Rev. Mod. Phys.* **80**, 885 (2008).  
<sup>2</sup> M. Greiner, O. Mandel, T. Esslinger, T. W. Hänsch, and I. Bloch, *Nature (London)* **415**, 39 (2002).  
<sup>3</sup> S. Diehl, M. Baranov, A. J. Daley, and P. Zoller, *Phys. Rev. Lett.* **104**, 165301 (2010); *Phys. Rev. B* **82**, 064509 (2010); *Phys. Rev. B* **82**, 064510 (2010).  
<sup>4</sup> Y.-W. Lee and M.-F. Yang, *Phys. Rev. A* **81**, 061604(R) (2010).  
<sup>5</sup> A. J. Daley, J. Taylor, S. Diehl, M. Baranov, and P. Zoller, *Phys. Rev. Lett.* **102**, 040402 (2009).  
<sup>6</sup> M. Roncaglia, M. Rizzi, and J. I. Cirac, *Phys. Rev. Lett.* **104**, 096803 (2010).  
<sup>7</sup> L. Mazza, M. Rizzi, M. Lewenstein, and J. I. Cirac, *Phys. Rev. A* **82**, 043629 (2010).  
<sup>8</sup> S. Coleman and E. Weinberg, *Phys. Rev. D* **7** 1888 (1973); B. I. Halperin, T. C. Lubensky, and S.-K. Ma, *Phys. Rev. Lett.* **32**, 292 (1974).  
<sup>9</sup> L. Bonnes and S. Wessel, *Phys. Rev. Lett.* **106**, 185302

(2011).

<sup>10</sup> M. Dalmonde, M. Di Dio, L. Barbiero, and F. Ortolani, *Phys. Rev. B* **83**, 155110 (2011).  
<sup>11</sup> K. P. Schmidt, J. Drier, A. Läuchli, and F. Mila, *Phys. Rev. B* **74**, 174508 (2006).  
<sup>12</sup> Because the excitation energies of the single-particle and the single-hole states can be calculated analytically, there exist exact expressions of the phase boundaries for the *continuous* MI-ASF transitions. That is,  $\mu_{c,0\text{MI-ASF}} = -zt$  for the  $n = 0$  state, while  $\mu_{c,2\text{MI-ASF}} = 2zt - 1 + 2zV$  for the  $n = 2$  state. Here  $z$  is the coordination number. Our numerical data on finite systems for these continuous transitions agree with the analytical results.  
<sup>13</sup> For the  $V = 0$  case, the phase boundaries of the continuous transitions achieved by ED coincide with the results evaluated by the SSE QMC algorithm implemented with a two-loop update scheme<sup>14</sup> for system size  $N_s = 24 \times 24$  and temperature  $T = 0.001$ , while the estimated first-order transition points somewhat deviate from the QMC values. This shows that the present ED analysis can indeed give correct phase boundaries.

- <sup>14</sup> K.-K. Ng and M.-F. Yang, Phys. Rev. B. **83**, 100511 (2011).
- <sup>15</sup> Y. Ohta, A. Nakauchi, R. Eder, K. Tsutsui, and S. Maekawa, Phys. Rev. B. **52**, 15617 (1995).
- <sup>16</sup> P. W. Leung, Phys. Rev. B. **65**, 205101 (2002).